A network-based structure-preserving dynamical model for the study of cascading failures in power grids

Xinkai Fan[a,b], Ekaterina Dudkina[b], Lucia Valentina Gambuzza[c], Mattia Frasca[c], Emanuele Crisostomi[b]

[a] *State Key Laboratory of Electrical Insulation and Power Equipment, Xi'an Jiaotong University, Xi'an, China*
[b] *Department of Energy, Systems, Territory and Constructions Engineering, University of Pisa, Pisa, Italy*
[c] *Department of Electrical Electronic and Computer Engineering, University of Catania, Catania, Italy*

Abstract

In this work we show that simple classic models of power grids, albeit frequently utilized in many applications, may not be accurate or reliable for investigating cascading failures problems. For this purpose, we develop a novel model, based on a structure-preserving approach, to obtain a network-based description of a power grid, where nodes correspond to generators and buses, while the links correspond to the physical lines connecting them. In addition, we also consider classic voltage and frequency protection mechanisms for lines and buses. Considering the Italian power grid as a case study of interest, we then investigate the propagation of an initial failure of any line of the power system, and compare the predicted impact of the failure according to the simpler and the more accurate model. In particular, it can be observed that more realistic models are crucial to determine the size of the cascading failure, as well as the sequence of links that may be involved in the cascade.

Keywords: Power grids, complex networks, failures

Email addresses: fanxinkai@stu.xjtu.edu.cn (Xinkai Fan), ekaterina.dudkina@phd.unipi.it (Ekaterina Dudkina), lucia.gambuzza@dieei.unict.it (Lucia Valentina Gambuzza), mattia.frasca@dieei.unict.it (Mattia Frasca), emanuele.crisostomi@gmail.com (Emanuele Crisostomi)

1. Introduction

1.1. Motivation

The increasing amount of power generation from renewable sources with its associated intrinsic uncertainty, together with the ever-decreasing inertia of conventional generation units, are driving the interest of research communities in improving the resilience of current power grids, and in predicting possible occurrences of cascading failures. For the latter purpose, current practises involve the utilization of massive Monte Carlo simulations of a very detailed electromechanical description of the devices in the power grid to predict the behaviour of power grids as a consequence of particularly unlucky sequences of faults. Such *brute-force* approaches suffer from obvious limitations in terms of required computational burden, due to the combinatorial nature of the problem, and can not guarantee resilience of the network under unlikely and not tested sequences of faults. Accordingly, other researchers have investigated the cascading failure problem in a simplified framework, where only the topology of the power network is considered, or where simple ordinary differential equations (ODEs) are used to model loads, generators and the connecting lines. While such methods have the advantage to quickly provide an insight of critical lines that may indeed trigger cascading failures, yet the ability of such models to realistically describe complex physical systems such as power grids is usually limited, and the value of their predictions may be regarded as questionable.

There is somewhat a gap between very simple static, or ODE-based, models, and more sophisticated Monte Carlo power grid simulations, and whether cascading failures may be realistically predicted based on analytic tools remains today an open problem. Besides, the aforementioned ever increasing presence of inertia-less devices on the generation side is further demanding for this problem to be addressed in a timely manner. Accordingly, the objective of this paper is to develop a novel model for power systems, that may serve as a reasonable trade-off between unrealistically simplistic models and sophisticated power systems simulators, and to assess the ability of simpler models to make realistic

predictions of after-faults evolutions.

1.2. State of the art

Due to its practical relevance, the problem of modeling cascading failures in power grids has attracted a lot of interest in different scientific communities. Previous approaches to the study of the problem may be classified into three classes: 1) network-based structural approaches; 2) techniques based on either DC or AC power flow calculations; 3) models explicitly incorporating the dynamics of the power grids.

The first class includes a series of models that do not incorporate any description of the electrical phenomena taking place in the power grid, but only consider the structural properties of the network of interconnections [1, 2, 3, 4]. All these works assume that a failure may be modeled by removing a component of the network, and investigate what happens in terms of the new power flows after the failure. Different assumptions are however considered to model the loads, either at the level of a node [2, 1], or of an edge of the network [1, 4]. Other approaches are based on percolation theory focusing either on cascades triggered by node removals [5] or link failures [6]. More sophisticated interdependencies between different structures taking into account, for instance, the physical network of the power grid and the overlying communication network have been also addressed using model-based multi-layer structures in [7].

The second class comprises approaches that take into account the physical properties of the power grid, but limited to the steady-state equilibrium. They consider the power flows obtained by solving the DC or AC power flow equations [8, 9, 10, 11, 12]. These models, relying on a quite simple but tractable description of the electrical mechanisms underlying power grids, prompt for the definition of optimization-based methods for the identification of the lines leading to the worst-case cascading failures [13].

The third class comprises models that explicitly take into account the dynamics of the electro-mechanical phenomena occurring in the power grid. The level of description of these phenomena can vary significantly, often, simplified

models are applied to provide a coarse-grained description of the dynamics of the power grid [14, 15]. This approach, however, could suffer from oversimplification of the dynamics of the power grid, leading to under- or over-estimates of the cascades occurring in the power grid.

1.3. Contribution

The first contribution of this paper is to introduce a novel model for the study of cascading failures in power systems. The model is intended to provide a trade-off between unrealistically simplistic models and sophisticated power system simulators. With respect to the dynamical models introduced in [14, 15], our paper proposes a different model for the power grid. In fact, while Ref. [14] uses a Hamiltonian-like system model and Ref. [15] a model based on synchronous machines, in our work we consider a network-based, structure-preserving model. In addition, our model explicitly incorporates several protection mechanisms for the line and the bus which have not been considered in the two above mentioned papers. Then, the second contribution is to assess to ability of simpler models to accurately predict and describe possible cascading failures.

2. A structure-preserving dynamic model of failures

We now illustrate the proposed model for simulating power systems. As mentioned in the introductory section, the model was chosen to conveniently represent a trade-off between too simplistic ODE-based models and too sophisticated power system simulators. In particular, we now first describe the model adopted for representing nominal operation of the power grid, which is inspired by the classic structure-preserving model of [16], and in the following section we describe the protection mechanisms considered in our model.

2.1. Power System Model

Let us consider a power network having N_0 buses and N_g generators, and let us add fictitious buses to represent the internal generation voltages, such that the augmented network has $N = N_0 + N_g$ nodes. Let $\delta_g(t)$ with $g = 1, \ldots, N_g$

denote the rotor angle of the g-th generator at time t, $\omega_g(t)$ its angular speed relative to the reference frame given by the power line frequency $\Omega = 2\pi f$, with $f = 50Hz$ or $f = 60Hz$, and let $\theta_i(t)$ with $i = 1, \ldots, N$ denote the i-th bus angle. Without lack of generality, let us enumerate the buses so that the first N_g (i.e., with indices $i = 1, \ldots, N_g$) corresponds to the fictitious buses of the generators, while the remaining indices (i.e., $i = N_g + 1, \ldots, N$) correspond to load buses. For simplicity of notation, in the following we drop the time dependency when not necessary.

The dynamics of the generators is described by the swing equation:

$$\begin{aligned} \dot{\delta}_g &= \omega_g \\ M_g \dot{\omega}_g &= P_{M_g} - \frac{E_g V_g}{X_g} \sin(\delta_g - \theta_g) - D_g \omega_g \end{aligned} \tag{1}$$

with $g = 1, \ldots, N_g$. Here, M_g is the inertial term associated with the g-th generator, D_g is the damping constant, X_g is the (fictitious) generator internal reactance, P_{M_g} is the mechanical power, E_g is the generator voltage, and V_g is the bus voltage. Note that, thanks to the adopted labeling for buses, generator g is only connected to bus $i = g$.

Synchronous generators are usually equipped with governors that can change the input mechanical power to help to stabilize the system's frequency (often referred to as "primary frequency control"). There are many different standard governor models [17] for thermal and hydro generator in the detailed power system dynamic simulation. In this paper, a simplified governor model is used for the convenience of calculation. This module simplifies the whole governor dynamic into a first - order delay module. The governor model is presented in Fig. 1, where $P_{M_g(0)}$ is the pre-fault steady-state mechanical power, $P_{M_g(max)} = 1.2P_{M_g(0)}$ and $P_{M_g(min)} = 0.8P_{M_g(0)}$ are the maximum and minimum allowable input mechanical power, $K = 32$ and $T = 2$ are proportionality coefficient and time constant, respectively.

The transmission lines are modeled assuming that active power losses are negligible, and, hence, the admittance of the generic line (i, j) can be approximated by only its imaginary part B_{ij}, i.e., neglecting the line resistance. Taking

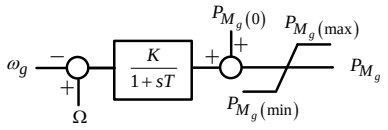

Figure 1: Simplified governor model.

this into account, the equations for the buses are given by the following algebraic constraints:

$$\begin{aligned} 0 &= P_{d_i} - \sum_{j=1}^{N} B_{ij} V_i V_j \sin(\theta_i - \theta_j) \\ 0 &= Q_{d_i} + \sum_{j=1}^{N} B_{ij} V_i V_j \cos(\theta_i - \theta_j) \end{aligned} \tag{2}$$

with $i = 1, \ldots, N$. Here, B_{ij} is the generic coefficient of the admittance matrix of the augmented network. P_{d_i} and Q_{d_i} represent the active and reactive power of load i, and they are modelled assuming they depend on the voltage of the node, as in classic ZIP (or polynomial) load models (see for instance [18, 19]). These models combine together the constant impedance (Z), constant current (I) and constant power (P) terms as follows:

$$\begin{aligned} P_{d_i} &= P_{d_i,0} \left(K_Z \left(\frac{V_i}{V_{i,0}} \right)^2 + K_I \frac{V_i}{V_{i,0}} + K_P \right) \\ Q_{d_i} &= Q_{d_i,0} \left(K_Z \left(\frac{V_i}{V_{i,0}} \right)^2 + K_I \frac{V_i}{V_{i,0}} + K_P \right) \end{aligned} \tag{3}$$

where $P_{d_i,0}$, $Q_{d_i,0}$ and $V_{i,0}$ are the values at the initial operating conditions, and K_Z, K_I, and K_P are appropriate non-negative coefficients, weighting the constant impedance, constant current and constant power terms. In our simulations we have set $K_Z = K_I = 0.5$, and $K_P = 1 - K_Z - K_I = 0$.

All together, equations (1-3) form a system of differential-algebraic equations (DAEs) that describe the dynamics of the power grid. This system is integrated in MATLAB using the ode15s DAEs solver, deriving the evolution of the variables $\delta_g(t)$, $\omega_g(t)$, $V_i(t)$ and $\theta_i(t)$ with $g = 1, \ldots, N_g$ and $i = 1, \ldots, N$.

2.2. Models of Faults

2.2.1. Line Failures

We consider that each line of the power grid is equipped with two protection systems: to deal with tie-line flow limits among regions (overload protection) and out-of-step protection. If one of the two protection devices is triggered, then the line is tripped from the rest of the network.

In particular, we assume that a tie-line constraint violation (an overload fault) occurs when the power flow on a line exceeds a percentage of the line capacity for a period of time larger than τ_{lo}. More specifically, the flow along the line connecting bus i and bus j is given by $F_{ij}(t) = V_i V_j B_{ij} \sin(\theta_j(t) - \theta_i(t))$. The capacity C_{ij} of a line is defined as a fraction of the maximum flow, which is given by B_{ij}, i.e., $C_{ij} = \alpha B_{ij}$, where $\alpha \in [0, 1]$ is a tunable parameter (see [15]). Accordingly, an overload condition is said to occur at a time $t = \bar{t}$ when

$$|F_{ij}(t)| > \alpha B_{ij}, \forall t \in [\bar{t} - \tau_{lo}, \bar{t}]. \tag{4}$$

In addition, we have considered a further protection mechanism to account for out-of-step events. This out-of-step protection mechanism is commonly used to split the network into several components in case of such events [20, 21]. Real out-of-step protection mechanisms are often based on the evaluation of the impedance at one terminal of a transmission line, calculated as the ratio between the voltage and the current measured at the node. Then, since during a swing this impedance is not constant, the protection mechanism evaluates the variation of the measured impedance to eventually trip the line. Here we take a simplified implementation approach by checking whether the phase difference (in absolute value) of the bus angles exceeds 2π, i.e., $|\theta_j - \theta_i| > 2\pi$. When this condition is satisfied, then we assume that the out-of-step protection system triggers the disconnection of the line [20].

2.2.2. Failures of Load Buses

Bus failures may either occur at load or generator buses. Let us first discuss the case of a load bus: we assume that each load bus is equipped with both

voltage and frequency protection systems. These systems may determine either a full or partial tripping of the bus. In particular, here we assume that a load bus is generally only partially tripped, whereas it is fully tripped only in the case of a significant overvoltage. Each protection mechanism is associated with an inequality condition, and the protection mechanism is triggered if the condition is violated for a given interval of time.

Consider a bus i and its associated bus voltage V_i. Two mechanisms are implemented accounting respectively for undervoltage load shedding control, that, in power systems, is used to prevent voltage collapse [22], and for overvoltage tripping that is used to simulate the damage caused by overvoltage and protect the device [23]. For the overvoltage protection mechanism, we consider two trigger conditions depending on the severity of the overvoltage. A first milder condition is given by:

$$V_i(t) > r^L_{hv,1} V_i(0), \forall t \in [\bar{t} - \tau^L_{hv,1}, \bar{t}] \tag{5}$$

where the term $r^L_{hv,1} V_i(0)$ represents the smaller threshold value and $\tau^L_{hv,1}$ the time delay before the protection mechanism comes into play. As it can be noticed, the threshold depends on the initial value of the bus voltage and a constant parameter $r^L_{hv,1}$. If this condition is met, then the load bus is partially tripped. A second overvoltage protection mechanism regulates the most critical condition as follows:

$$V_i(t) > r^L_{hv,2} V_i(0), \forall t \in [\bar{t} - \tau^L_{hv,2}, \bar{t}] \tag{6}$$

where $r^L_{hv,2}$ and $\tau^L_{hv,2}$ have an analogous meaning to that of Equation (5), but now the load bus is fully tripped when this condition is satisfied. Obviously, $r^L_{hv,2} > r^L_{hv,1}$ and $\tau^L_{hv,2} < \tau^L_{hv,1}$, so that the second mechanism is activated when a higher overvoltage is experienced.

In an analogous way, we include a protection mechanism for the undervoltage case, associated with the following condition:

$$V_i(t) < r_{lv}^L V_i(0), \forall t \in [\bar{t} - \tau_{lv}^L, \bar{t}] \tag{7}$$

where the term $r_{lv}^L V_i(0)$ represents the low voltage threshold and τ_{lv}^L the corresponding delay before the protection system should be triggered. If this condition is satisfied, then the load bus is partially tripped.

In addition to the voltage protection systems, we also consider frequency protection systems in each load bus of the power grid. In fact, in power systems, load buses are often equipped with low-frequency load shedding control [24], which aims at maintaining a stable system frequency, eventually tripping the load as a function of the deviation from the nominal frequency. Similarly, loads could be also equipped with over-frequency protection mechanism to deal with scenarios where loads are sensitive to the frequency and could require tripping in case that the oscillations at a frequency higher than the nominal one arise [25]. However, not to increase further the burden to the whole system, over-frequency events do not lead to load tripping in our model.

To model these protection mechanisms, we consider the instantaneous frequency of load buses defined as $\tilde{\omega}_i(t) = \dfrac{d\theta_i(t)}{dt}$ and check the condition

$$\tilde{\omega}_i(t) < \omega_{lf}^L, \forall t \in [\bar{t} - \tau_{lf}^L, \bar{t}] \tag{8}$$

for low frequency protection. The parameter ω_{lf}^L represent the threshold for underfrequency protection, and τ_{lf}^L the associated delays for the protection to be activated. When the above condition is satisfied, then the load bus is partially tripped. In particular, in case of partial tripping, the node active and reactive powers are set to a fraction of their values as determined by the ZIP model, that is:

$$\begin{aligned} P_{d_i} &= \alpha_k^L P_{d_i,0} \left(K_Z \left(\frac{V_i}{V_{i,0}} \right)^2 + K_I \frac{V_i}{V_{i,0}} + K_P \right) \\ Q_{d_i} &= \alpha_k^L Q_{d_i,0} \left(K_Z \left(\frac{V_i}{V_{i,0}} \right)^2 + K_I \frac{V_i}{V_{i,0}} + K_P \right) \end{aligned} \tag{9}$$

here the index k labels the different protection mechanisms considered, i.e., $k = \{hv_1, hv_2, lv, lf\}$. For each one of them, α_k^L indicates the fraction of partial tripping of the load, whose value thus depends on the specific event that caused the partial tripping. For the undervoltage and underfrequency protection mechanisms, the amount of tripping depends on how much the value (voltage or frequency) differs from the threshold. In particular, for α_{lv}^L we have considered:

$$\alpha_{lv}^L = \begin{cases} 0.9 & \texttt{if } 0 < V_{lv}^L - V_i(t) \leq 0.02 \\ 0.85 & \texttt{if } 0.02 < V_{lv}^L - V_i(t) \leq 0.04 \\ 0.8 & \texttt{if } 0.04 < V_{lv}^L - V_i(t) \leq 0.07 \\ 0.75 & \texttt{if } 0.07 < V_{lv}^L - V_i(t) \leq 0.09 \\ 0.7 & \texttt{if } V_{lv}^L - V_i(t) > 0.09 \end{cases}, \tag{10}$$

while for α_{lf}^L we have

$$\alpha_{lf}^L = \begin{cases} 0.95 & \texttt{if } 0 < \omega_{lf}^L - \tilde{\omega}_i(t) \leq 0.005 \\ 0.9 & \texttt{if } 0.005 < \omega_{lf}^L - \tilde{\omega}_i(t) \leq 0.01 \\ 0.85 & \texttt{if } 0.01 < \omega_{lf}^L - \tilde{\omega}_i(t) \leq 0.015 \\ 0.8 & \texttt{if } 0.015 < \omega_{lf}^L - \tilde{\omega}_i(t) \leq 0.02 \\ 0.75 & \texttt{if } 0.02 < \omega_{lf}^L - \tilde{\omega}_i(t) \leq 0.08 \\ 0.7 & \texttt{if } \omega_{lf}^L - \tilde{\omega}_i(t) > 0.08 \end{cases}. \tag{11}$$

The parameters used for the protection mechanisms for the load buses are reported in Table 1.

$r_{hv,1}^L$	1.1	$\tau_{hv,1}^L$	1	$\alpha_{hv,1}^L$	0.7
$r_{hv,2}^L$	1.5	$\tau_{hv,2}^L$	0.1	$\alpha_{hv,2}^L$	0
V_{lv}^L	0.87	τ_{lv}^L	0.5	α_{lv}^L	Eq. (10)
ω_{lf}^L	-0.02	τ_{lf}^L	0.5	α_{lf}^L	Eq. (11)

Table 1: Values of the parameters used in the structure-preserving dynamical model for the protection mechanisms for load nodes.

In the case of the simultaneous activation of more than one protection mechanism, then the resulting amount of tripping is determined by all the triggered

mechanisms. For instance, if the low frequency and low voltage shedding events occur at the same node, then, the load is tripped with a factor equal to $\alpha^L_{lv} \cdot \alpha^L_{lf}$. Finally, we note that full tripping of the load nodes corresponds to set to zero the active and reactive power, that is, $P_{d_j} = 0$, and $Q_{d_j} = 0$.

2.2.3. Failures of Generation Buses

Protection mechanisms for the failure of generation buses are very similar to those for the failure of load buses described in Section 2.2.2. Let us starting with the overvoltage protection mechanism, which aims at preventing generator over-flux and insulation damage [25]. Two overvoltage conditions are considered and in both cases they result in fully tripping the node (which corresponds now to a generator bus). The first condition is given by

$$V_i(t) > r^G_{hv,1} V_i(0), \forall t \in [\bar{t} - \tau^G_{hv,1}, \bar{t}] \tag{12}$$

where the term $r^G_{hv,1} V_i(0)$ represents the smaller threshold value and $\tau^G_{hv,1}$ the time delay before the protection mechanism comes into play. A second overvoltage protection mechanism occurs when the following critical condition is met:

$$V_i(t) > r^G_{hv,2} V_i(0), \forall t \in [\bar{t} - \tau^G_{hv,2}, \bar{t}] \tag{13}$$

where $r^G_{hv,2}$ and $\tau^G_{hv,2}$ have an analogous meaning to that of Equation (12). Obviously, $r^G_{hv,2} > r^G_{hv,1}$ and $\tau^G_{hv,2} < \tau^G_{hv,1}$, so that the second mechanism is activated when a higher overvoltage (in a smaller time) is experienced.

For undervoltage events, we do not equip an undervoltage protection that directly trips the generator. In fact, undervoltage events usually do not cause direct damage to the generator, such that, in real power plants, these events typically generate warning signals for the plant operator without tripping the generator. On the other hand, undervoltage events may cause overcurrent which can be handled by the overcurrent protection mechanism considered in our paper [25].

Two thresholds are considered again for overfrequency events occurring at generators buses, to take into account milder and more critical events. Accordingly, at the i-th bus generator we have a first protection mechanism that triggers to maintain the system frequency stability, and acts by partially tripping the generator by a quantity which depends on the intensity of the event [26]. The triggering condition is expressed by:

$$\omega_i(t) > \omega^G_{hv,1}, \forall t \in [\bar{t} - \tau^G_{hf,1}, \bar{t}] \tag{14}$$

where $\omega^G_{hf,1}$ is the smaller threshold value and $\tau^G_{hf,1}$ the time delay before the protection mechanism comes into play. If this condition is met, then the generator bus is partially tripped. A second overfrequency protection mechanism regulates the most critical condition as follows:

$$\omega_i(t) > \omega^G_{hf,2}, \forall t \in [\bar{t} - \tau^G_{hf,2}, \bar{t}] \tag{15}$$

where $\omega^G_{hf,2}$ and $\tau^G_{hf,2}$ have an analogous meaning to that of Equation (14), but now the generator bus is fully tripped when this condition is satisfied. Obviously, $\omega^G_{hf,2} > \omega^G_{hf,1}$ and $\tau^G_{hf,2} < \tau^G_{hf,1}$, so that the second mechanism is activated to protect the generator itself [25], when a higher overfrequency is experienced. On the other hand, the underfrequency case is usually also critical, and we assume that a full tripping of the generator bus occurs when an underfrequency situation is observed for a long enough time, as follows:

$$\tilde{\omega}_i(t) < \omega^G_{lf}, \forall t \in [\bar{t} - \tau^G_{lf}, \bar{t}] \tag{16}$$

where as usual ω^G_{lf} is the low frequency threshold and τ^G_{lf} is the corresponding delay before the protection system is triggered.

For generation nodes, partial tripping is implemented setting the active power to a fraction of its value, that is:

$$P_{d_i} = \alpha^G_k P_{d_i,0} \tag{17}$$

In the case of overfrequency events, then the amount of tripping is function of the difference between the instantaneous frequency $\tilde{\omega}_i(t)$ and the threshold

value ω_{hf}^G, according to the following law:

$$\alpha_{hf}^G = \begin{cases} 0.95 & \texttt{if } 0 < \omega_{hf}^G - \tilde{\omega}_i(t) \leq 0.005 \\ 0.9 & \texttt{if } 0.005 < \omega_{hf}^G - \tilde{\omega}_i(t) \leq 0.01 \\ 0.85 & \texttt{if } 0.01 < \omega_{hf}^G - \tilde{\omega}_i(t) \leq 0.015 \\ 0.8 & \texttt{if } 0.015 < \omega_{hf}^G - \tilde{\omega}_i(t) \leq 0.02 \\ 0.75 & \texttt{if } 0.02 < \omega_{hf}^G - \tilde{\omega}_i(t) \leq 0.09 \\ 0 & \texttt{if } 0.09 < \omega_{hf}^G - \tilde{\omega}_i(t) \end{cases} . \quad (18)$$

The parameters set in our simulations for the protection mechanisms at the generation buses are given in Table 2.

$r_{hv,1}^G$	1.1	$\tau_{hv,1}^G$	10	$\alpha_{hv,1}^G$	0
$r_{hv,2}^G$	1.5	$\tau_{hv,2}^G$	0.1	$\alpha_{hv,2}^G$	0
ω_{hf}^G	0.01	τ_{hf}^G	0.5	α_{hf}^G	see Eq. (18)
ω_{lf}^G	-0.04	τ_{lf}^G	1	α_{lf}^G	0

Table 2: Values of the parameters used in the structure-preserving dynamical model for the protection mechanisms for generation nodes.

3. An alternative simpler model for cascading failures in power grids

In this Section, we briefly discuss an alternative model to study cascading failures in power grids. We start with the dynamical model presented in [15] and, then, as an example of models based on a quasi-static approach, we discuss the case study derived from the dynamical model of Ref. [15].

3.1. Synchronous-machine dynamic model

The model considered in [15] is based on a synchronous-machine representation of the power grid. According to this representation, each node of the grid is modeled as a rotating machine whose dynamics is described by a swing equation. In this model, the number of nodes, N, corresponds to that of the buses, N_0. The network nodes are divided into loads or generators according to the sign of the power P_i, which can be either positive, $P_i > 0$, for nodes that,

injecting the power into the system, act as generators, or negative, $P_i > 0$, for nodes that, absorbing the power from the system, act as loads. Each node is characterized by a swing equation describing the dynamics of the mechanical rotor angle $\theta_i(t)$, that corresponds to the voltage phase angle, and by its angular velocity $\omega_i = d\theta_i/dt$, with $i = 1, \ldots, N$. These quantities are expressed relative to the rotating reference frame with velocity $\Omega = 2\pi f$, where $f = 50Hz$ or $f = 60Hz$.

To derive a set of simplified system equations, a series of specific assumptions that simplify the power flow equations: i) the voltage amplitudes V_i are assumed to be constant; ii) the ohmic losses are assumed to be negligible; iii) the variations in the angular velocities, ω_i, are considered to be small compared to the reference Ω. Under these assumptions, the system behavior is modelled by the following swing equations:

$$\begin{aligned} &\frac{d\theta_i}{dt} = \omega_i \\ &I_i \frac{d\omega_i}{dt} = P_i - \gamma_i \omega_i + \sum_{j=1}^{N} K_{ij} \sin(\theta_j - \theta_i) \end{aligned} \tag{19}$$

where I_i represents the inertia associated to the rotating machine in node i, γ_i its damping constant, and K_{ij} the elements of a weighted adjacency matrix describing the topology of the power grid. The terms K_{ij} are related to the node voltages by the relationship $K_{ij} = B_{ij} V_i V_j$.

The model presented in [15] only considers line failures, as modeled by the condition (4). In particular, in [15] for most of the scenarios analyzed this condition is checked instantaneously, i.e., with $\tau_{lo} = 0$, but some selected case studies with $\tau_{lo} > 0$ are presented in the Supplementary Material. In the following, we consider this model with $\tau_{lo} = 0$.

4. Simulation results

4.1. Case study

In our simulations, we consider a simplified description of the Italian high-voltage (380kV) power grid [27], which consists of $N = 127$ nodes (34 generators

and 93 loads) connected by 171 edges, as depicted in Fig. 2. Since we are only interested in comparing different models, here for simplicity we assume that the network is undirected and unweighted, that is, $B_{ij} = B_{ji} = B$. Correspondingly, in the SM model we have $K_{ij} = ka_{ij}$, where $a_{ij} = \{0, 1\}$ are the elements of the adjacency matrix encoding the network connectivity. Similar assumptions have been considered in other works, e.g., [28, 29, 30, 31, 32]. Here, we assume $B = 0.04$ ($k = 25$) which guarantees that, in the absence of faults, the network is synchronized. In addition, we consider $\alpha = 0.6$. Finally, the damping parameter D_g and the (fictitious) generator internal reactance X_g have been assumed to be homogenous along the generation nodes and set to $D_g = D = 0.1$ and $X_g = X = 0.0547$.

In the following we analyze the effect of removing a single line of a network (accounting for a fault due to some exogenous event), starting from an equilibrium condition. As a consequence of the initial fault, the network is no more at the equilibrium and, depending on its dynamical evolution, cascading failures can be generated. For each initial fault, we thus monitor which lines are subject to subsequent failures.

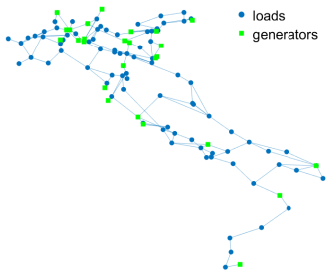

Figure 2: Schematic representation of Italian high-voltage (380kV) power grid [27].

4.2. Different predictions of cascade failures

A first observation deriving from our simulations is that the SP (Structure-Preserving) and the SM (Synchronous-Machine) models make different predic-

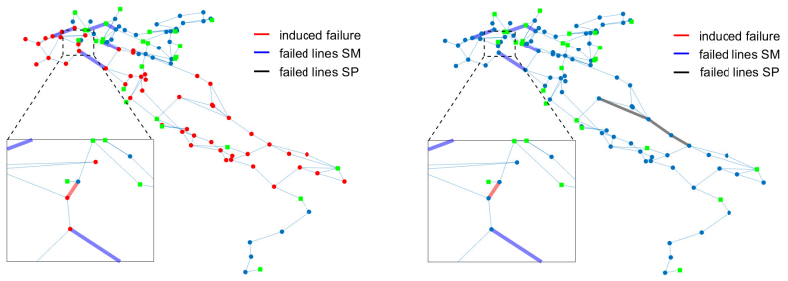

(a) (b)

Figure 3: Cascading failures induced in the Italian power grid by an initial fault in link 17 (highlighted in red), according to the SP and SM model: (a) with protection mechanisms enabled; (b) without protection mechanisms.

tions about possible cascading failures. As a specific example, let us consider the case that a fault occurs at link 17, highlighted in red in Fig. 3. As a consequence of the initial fault of this line, the SP model does not produce any other failure; however the loads of 59 buses, which are highlighted in red in Fig. 3(a), are reduced with different intensities by the low voltage protection mechanism. Conversely, for the same initial fault, the SM model predicts a cascading failure that involves six lines, highlighted in light blue in Fig. 3(a). It is also important to note that in the absence of protection mechanisms, the two models still lead to different results. In particular, Fig. 3(b) illustrates the outcome of the SP model in absence of protection mechanisms, showing that different failures are predicted.

From the comparison of Fig. 3(a) and Fig. 3(b), it is also possible to appreciate the effect of the protection mechanisms that are able to eliminate the cascading failures following the fault of line 17, as without such protection devices there are three lines that fail. This indicates that the protection mechanisms are actively involved in reducing the size of the cascade and neglecting them may yield to overestimate it.

As a second example, we consider an initial fault located in line 107. Again,

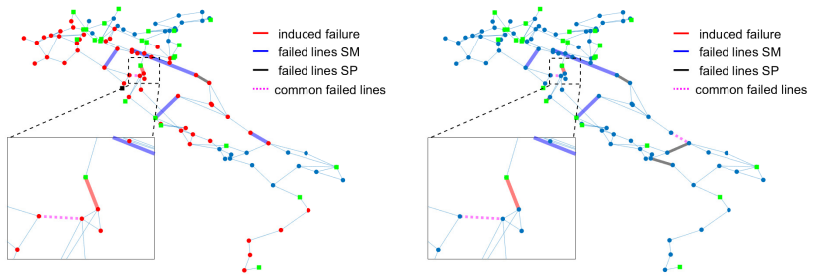

(a) (b)

Figure 4: Cascading failures induced in the Italian power grid by an initial fault in link 107 (highlighted in red), according to the SP and SM model: (a) with protection mechanisms enabled; (b) without protection mechanisms.

the SP and the SM model provide different predictions, which are shown in black and blue respectively in Fig. 4, but, in this case, both models predict a failure in line 105 (depicted with pink dashed segment). Without protection mechanisms, instead, the lines that are predicted to fail in the SP and SM model are two (lines 105 and 142).

4.3. Criticality of lines in the Italian power grid

We now assess the criticality of single lines of the Italian power grid, in terms of the size of the cascading failure that is triggered, if any, by the removal of the line. Roughly speaking, a line is denoted as critical if its removal triggers the failure of a large number of lines. Again, different models provide different assessments. In particular, the SP model with protection mechanisms (illustrated in Fig. 5(a)) predicts that 8 of the 171 lines induce subsequent cascades. All of these lines are mildly critical as they produce a cascade with less than 5 other failures, and the two most critical lines give rise to 2 subsequent failures. In addition, there are 3 load nodes with degree one (i.e., that they are connected to a single other node), such that the failure of the single line linking them to the rest of the network obviously results in a critical disconnection from the power grid, and the power demand of these nodes cannot be satisfied.

As anticipated while discussing the behavior of lines 17 and 107, the presence of protection mechanisms drastically reduces the size of the cascading failures. This result can be appreciated in Fig. 5(b) that corresponds to the case when protection mechanisms are not activated. In this case 10 lines are causing a cascade failure and the size of the resulting cascade is bigger: two lines trigger a cascade of more than five lines and the overall 20 more lines fail. It is worth noticing that inducing a failure of line 39 causes a cascade with the protection mechanisms in force, but it does not lead to any line tripping when the protection is off. This single case reveals that, for a more realistic scenario, the parameters of the protection mechanisms need to be adjusted for each particular line to take into account the specific characteristics of a system made by different devices.

Finally, Fig. 5(c) shows the prediction of the SM model. Here, the difference is the number of lines leading to a cascade and the size of the cascade for each line. This is clear from figure Fig. 5(f) where 22 lines among the total 171 cause failures in the network. For nine of them the size of the cascade is less then five, while for the remaining ones the size of the cascade is between six and thirteen. The most critical cases are associated with a fault occurring at line 47, which yields a cascade of 12 lines, or at line 83 with a cascade of 13 lines. These two lines are represented in red in Fig. 5(c). It is worth noticing that, in both approaches, the lines leading to failures are located in the northern part of the power grid.

5. Conclusions

In this work, we developed a network-based, structure-preserving model for the investigation of cascading failures in power grids. The model describes the dynamics of the power grid with a system of differential-algebraic equations and incorporates several protection mechanisms for lines and buses. This approach provides a compromise between an accurate representation of the real system dynamics, but with a limited computational complexity. The model was then compared with a simpler static ODE model for a case study inspired by the

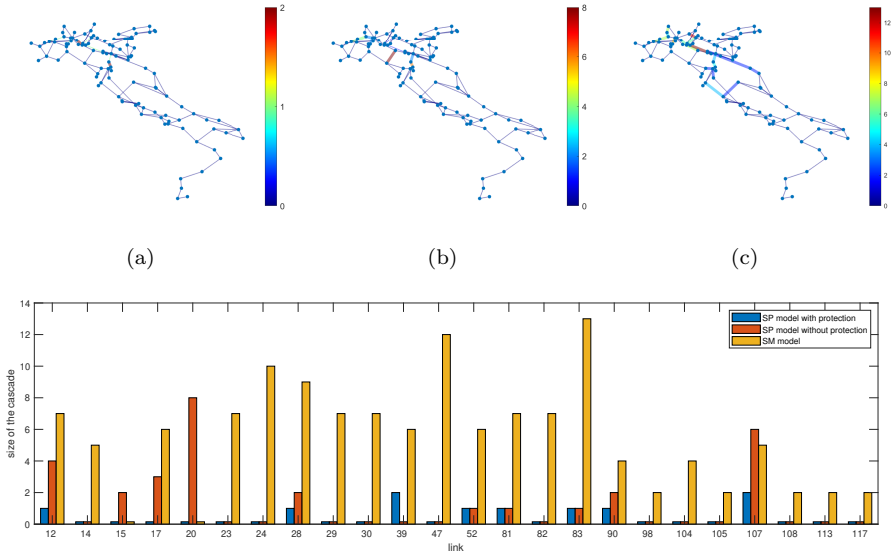

(a) (b) (c)

(d)

Figure 5: Size of the cascades triggered by faults at the lines of the Italian power grid: (a) SP model with protection mechanisms enabled; (b) SP model without protection mechanisms; (c) SM model; (d) comparison of the models.

Italian high-voltage power grid, in terms of cascading failures triggered by induced line outages. The comparison was performed for two operating modes of the proposed model: in the first one, line protections, as well as bus frequency and voltage protection mechanisms, were in force; in the second one, only line protections were enabled. In both cases, the results showed that simpler ODE models may not be reliable in performing the required task, as they tend to overestimate the size of the cascade and could lead to wrong predictions of after-fault impacts.

While the main purpose of this work was to highlight the weaknesses, in terms of poor reliability, of frequently used simplified models of power grids for investigating cascading failures, our future research interests include considering more realistic power grids, and introducing possible control strategies to mitigate the cascading failures.

Acknowledgements

This paper has been partially supported by the Italian Ministry for Research and Education through the Research Program PRIN 2017 (Grant 2017CWMF93, project VECTORS). The Authors would like to thank prof. Federico Milano, from the University College Dublin (UCD), for his valuable suggestions and comments on preliminary drafts of this manuscript.

References

[1] A. E. Motter, Cascade control and defense in complex networks, Physical Review Letters 93 (9) (2004) 098701.

[2] P. Crucitti, V. Latora, M. Marchiori, Model for cascading failures in complex networks, Physical Review E 69 (4) (2004) 045104.

[3] I. Dobson, B. A. Carreras, V. E. Lynch, D. E. Newman, Complex systems analysis of series of blackouts: Cascading failure, critical points, and

self-organization, Chaos: An Interdisciplinary Journal of Nonlinear Science 17 (2) (2007) 026103.

[4] Y. Zhang, O. Yağan, Optimizing the robustness of electrical power systems against cascading failures, Scientific reports 6 (2016) 27625.

[5] Z. Kong, E. M. Yeh, Resilience to degree-dependent and cascading node failures in random geometric networks, IEEE Transactions on Information Theory 56 (11) (2010) 5533–5546.

[6] H. Xiao, E. M. Yeh, Cascading link failure in the power grid: A percolation-based analysis, in: 2011 IEEE International Conference on Communications Workshops (ICC), IEEE, 2011, pp. 1–6.

[7] S. V. Buldyrev, R. Parshani, G. Paul, H. E. Stanley, S. Havlin, Catastrophic cascade of failures in interdependent networks, Nature 464 (7291) (2010) 1025–1028.

[8] P. Hines, E. Cotilla-Sanchez, S. Blumsack, Do topological models provide good information about vulnerability in electric power networks?, Chaos: An Interdisciplinary Journal of Nonlinear Science 20 (2010) 033122.

[9] S. Soltan, D. Mazauric, G. Zussman, Analysis of failures in power grids, IEEE Transactions on Control of Network Systems 4 (2) (2015) 288–300.

[10] H. Cetinay, S. Soltan, F. A. Kuipers, G. Zussman, P. Van Mieghem, Comparing the effects of failures in power grids under the ac and dc power flow models, IEEE Transactions on Network Science and Engineering 5 (4) (2017) 301–312.

[11] H. Cetinay, K. Devriendt, P. Van Mieghem, Nodal vulnerability to targeted attacks in power grids, Applied network science 3 (1) (2018) 34.

[12] J. Strake, F. Kaiser, F. Basiri, H. Ronellenfitsch, D. Witthaut, Non-local impact of link failures in linear flow networks, New Journal of Physics 21 (5) (2019) 053009.

[13] C. Zhai, H.-H. Zhang, G. Xiao, T.-C. Pan, An optimal control approach to identifying the worst-case cascading failures in power systems, IEEE Transactions on Control of Network Systems.

[14] C. L. DeMarco, A phase transition model for cascading network failure, IEEE Control Systems Magazine 21 (6) (2001) 40–51.

[15] B. Schäfer, D. Witthaut, M. Timme, V. Latora, Dynamically induced cascading failures in power grids, Nature communications 9 (1) (2018) 1–13.

[16] A. R. Bergen, D. J. Hill, A structure preserving model for power system stability analysis, IEEE transactions on power apparatus and systems (1) (1981) 25–35.

[17] I. Boldea, The Electric Generators Handbook - 2 Volume Set, 2005.

[18] J. Machowski, Z. Lubosny, J. W. Bialek, J. R. Bumby, Power system dynamics: stability and control, John Wiley & Sons, 2020.

[19] A. Arif, Z. Wang, J. Wang, B. Mather, H. Bashualdo, D. Zhao, Load modeling—A review, IEEE Transactions on Smart Grid 9 (6) (2017) 5986–5999.

[20] D. A. Tziouvaras, D. Hou, Out-of-step protection fundamentals and advancements, in: 57th Annual Conference for Protective Relay Engineers, IEEE, 2004, pp. 1–26.

[21] D. M. Paunescu, R. Balaurescu, H. E. Olovsson, Dynamic model based complex checking of out-of-step protections, in: 2009 IEEE Bucharest PowerTech, 2009, pp. 1–8. doi:10.1109/PTC.2009.5281881.

[22] C. Mozina, Undervoltage load shedding, in: 2007 Power Systems Conference: Advanced Metering, Protection, Control, Communication, and Distributed Resources, 2007, pp. 39–54. doi:10.1109/PSAMP.2007.4740897.

[23] C. J. Mozina, Protection of power plant transformers using digital technology, in: 1999 IEEE Transmission and Distribution Conference (Cat. No.

99CH36333), Vol. 1, 1999, pp. 421–432 vol.1. doi:10.1109/TDC.1999.755388.

[24] G. Zhang, Epri power system dynamics tutorial, Tech. rep., Electric Power Research Institute (EPRI) (2009).

[25] C37.96-2012 - IEEE Guide for AC Motor Protection (Revision of IEEE Std C37.96-2000) (2013). doi:10.1109/IEEESTD.2013.6468048.

[26] S. EIRGRID, Over frequency generation shedding schedule (summary report), Tech. rep., EIRGRID & SONI (2018).

[27] GENI—Global Energy Network Institute, Map of Italian electricity grid, https://www.geni.org/globalenergy/library/national_energy_grid/italy/italiannationalelectricitygrid.shtml, [Online; accessed 21-December-2020].

[28] V. Rosato, S. Bologna, F. Tiriticco, Topological properties of high-voltage electrical transmission networks, Electric Power Systems Research 77 (2) (2007) 99–105.

[29] G. Filatrella, A. H. Nielsen, N. F. Pedersen, Analysis of a power grid using a kuramoto-like model, The European Physical Journal B 61 (4) (2008) 485–491.

[30] L. Fortuna, M. Frasca, A. Sarra Fiore, A network of oscillators emulating the italian high-voltage power grid, International Journal of Modern Physics B 26 (25) (2012) 1246011.

[31] L. Tumash, S. Olmi, E. Schöll, Stability and control of power grids with diluted network topology, Chaos: An Interdisciplinary Journal of Nonlinear Science 29 (12) (2019) 123105.

[32] C. H. Totz, S. Olmi, E. Schöll, Control of synchronization in two-layer power grids, Physical Review E 102 (2) (2020) 022311.